Poly-2-oxazoline-Derived Polyurethanes: A Versatile Synthetic Approach to Renewable Polyurethane Thermosets

ENRIQUE DEL RIO, GERARD LLIGADAS, JUAN CARLOS RONDA, MARINA GALIA , VIRGINIA CADIZ

Departament de Quimica Analitica i Quimica Organica, Universitat Rovira i Virgili, Campus Sescelades,

Marcel·lí Domingo, s/n, 43007 Tarragona, Spain

ABSTRACT: 2-Nonyl-2-oxazoline and 2-(9-decenyl)-2-oxazoline have been copolymerized in different proportions by cationic ring-opening polymerization to obtain a series of random linear copolymers with tailored molecular weight and double bond functionality in the side chains. Thiol-ene addition of 2-mercaptoethanol has been used to produce a set of polyoxazoline–polyols under mild conditions and with quantitative double bond transformation. The polyols obtained in this way were reacted with methylene-bis(phenylisocyanate) to yield a series of amorphous and semicrystalline polyurethane networks. The thermal stability and the thermomechanical properties of these thermosets have been studied and related with the structure of the parent polyols.

KEYWORDS: cationic polymerization; polyoxazolines; polyurethanes; renewable resources

INTRODUCTION

The depletion of world oil pool, rising price of crude oil, and increased environmental concerns are pressurizing the scientists for the use of renewable natural resources in different fields of applications as they are ecofriendly and cost-effective materials.[1] In this regard, vegetable oils are one of the most promising renewable raw materials because of their availability, structural variety, and chemical versatility. Vegetable oils containing unsaturated fatty acids can be used in polymerizations to make biobased polymers.[2–5] Moreover, numerous fatty acids are now available with a high purity that makes them attractive for synthesis and they are also used as raw materials for the chemical industry.[6]

Polyurethanes (PUs) are one of the most important and versatile classes of polymers and can vary from thermosetting to thermoplastic materials. PUs exhibit better abrasion resistance, toughness, chemical resistance, and mechanical strength compared to other polymers such as polyesters and polyesteramides. Moreover, their mechanical, thermal, and chemical properties can be tailored by reactions with various isocyanates and polyols. Usually, both isocyanates and polyols are petroleum based, but in recent, years, vegetable oils, fatty acids and their derivatives have attracted significant attention as raw materials for the preparation of polyurethanes.[7] For natural oils and derivatives to be used as raw materials for polyol production, multiple hydroxyl functionality is required.[8] This can be accomplished by various strategies like the epoxidation of carbon–carbon double bonds and further oxirane ring opening with alcohols and other nucleophiles,[9,10] transesterification with multifunctional alcohols,[11,12] and hydroformylation or ozonolysis and subsequent reduction of the carbonyl groups.[13,14] Unfortunately, these strategies usually lead to complex mixtures of polyols with different hydroxyl content, molecular architecture, and molecular size. In a recent work, we prepared a set of polyether polyols for synthesis of PUs by polymerization of the methyl 9,10-epoxyoleate and subsequent controlled reduction of the pendant side ester groups.[15–17] This new strategy allowed an excellent control of the polyol hydroxyl content but failed in the control of the polyol molecular weight and molecular architecture due to the nature of the cationic and ionic-coordinative polymerizations used. On the contrary, the living nature of the cationic ring-opening polymerization (CROP) of 2-substituted-2-oxazolines allows the facile preparation of well-defined homopolymers and copolymers with an excellent control of their molecular weight, end group functionalities, and molecular architecture allowing an accurate control of the final properties.[18–24] Moreover, 2-oxazoline monomers can be readily prepared directly from the carboxylic acids or their nitrile derivatives following various synthetic pathways.[25–30] In this way, 2-oxazolines are excellent candidates to transform unsaturated carboxylic fatty acids in polymers with tailored structure and functionality. Copolymerization of saturated and unsaturated 2-oxazoline monomers allows the preparation of linear copolymers with prefixed molecular weights and the desired amount of pendant double bonds in a random or block arrangement.[31–33] Side chain double bond

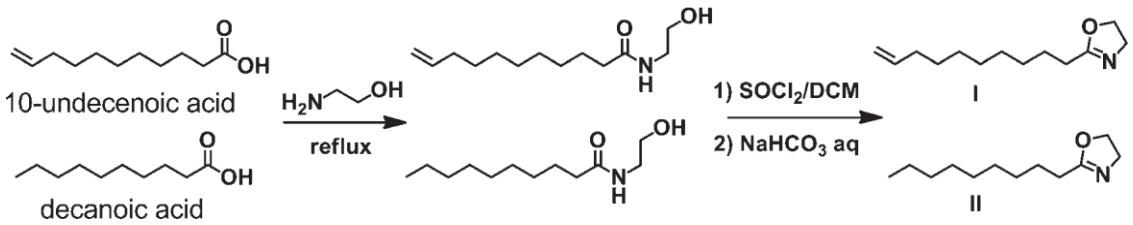

SCHEME 1 Synthesis of the oxazoline monomers I and II from 10-undecenoic and decanoic acids.

hydroxylation can be accomplished in different ways. Hydroboration/oxidation techniques have been applied successfully to polymers like polybutadiene,[34] poly(3-hydroxyundecen10-enoate),[35] poly(4-allyloxyphenyloxazoline),[36] and poly[2(9-decenyl)-2-oxazoline[37] but this approach needs low temperature conditions, a complex work up, and uses expensive reagents and strongly basic and oxidizing media what is undesirable in oxazoline-based polymers. Thiol-ene chemistry, which implies the free-radical addition of thiols onto double bonds, is a highly efficient tool that has been applied to polymer synthesis.[38–40] Click chemistry reactions have also been used in polyoxazolidines[41] and recently efficient thiol-ene modification of poly[2-(3-butenyl)-2-oxazoline],[42] poly[2-isopropyl/3-butenyl)-2-oxazoline,[43] and 2-oxazoline monomers[44] has been described.

This work describes the synthesis of random copolymers of 2-nonyl-2-oxazoline and 2-(9-decenyl)-2-oxazoline by CROP and its thiol-ene functionalization with 2-mercaptoethanol to produce a set of linear polyoxazoline–polyols under mild conditions, quantitative double bond transformation, and with control of the molecular weight and the hydroxyl content. The polyols obtained in this way were reacted with methylene-bis(phenylisocyanate) (MDI) to yield a series of polyurethane networks that were characterized by fluorescence infrared spectroscopy (FTIR), differential scanning calorimetry (DSC), thermogravimetric analysis (TGA), and thermodynamic mechanical analysis to establish the relationship of polyol structure–PU properties.

EXPERIMENTAL

Materials

2,2-Dimethoxy-2-phenylacetophenone (DMPA), 10-undecenoic acid, 2-mercaptoethanol, and MDI were purchased from Aldrich. Benzyl bromide and thionyl chloride were obtained from Fluka, and decanoic acid and ethanolamine were from Merck. Tetrahydrofuran (THF) and acetonitrile (ACN) from Aldrich were dried with sodium benzophenone and P_2O_5, respectively, and distilled immediately before use.

Synthesis of Monomers

2-(9-Decenyl)-2-oxazoline (I) and 2-nonyl-2-oxazoline (II) (Scheme 1) were synthesized starting from the corresponding acids and ethanolamine following general reported procedures.[45–48] The monomers were purified by fractional distillation over barium oxide under vacuum and stored under argon. The physical properties and spectral characteristics were in accordance with those described in the literature.[31,47] Purity was estimated as more than 98% by gas chromatography (GC).

Random Copolymerization

The copolymerization of I and II was carried out with benzyl bromide in anhydrous ACN at 100 °C for 24 h. Polymerizations and work-up were carried out following a similar procedure previously described.[48] In a typical copolymerization procedure, the appropriate amounts of I and II (see Table 1 for composition) (30 mmol) were placed in a flame-dried screw-capped shlenck flask under argon. Next, the necessary amount of anhydrous ACN was added to reach a 2 M solution. The mixture was stirred at room temperature and the necessary amount of anhydrous benzyl bromide was added by means a precision syringe. The polymerization mixture was heated and kept at 100 °C for 24 h. After cooling to 50 °C, the polymerization was stopped by adding few drops of 10% KOH solution in water and stirred for 1 h. The resulting solution was concentrated under vacuum; the residue was dissolved in ethyl acetate and the extracts were washed several times with brine, dried with anhydrous $MgSO_4$, and concentrated. The isolated polymer was dried at 40 °C under vacuum for 24 h. Results are summarized in Table 1.

^{1}H nuclear magnetic resonance (NMR) ($CDCl_3$, tetramethylsilane (TMS), δ in ppm): 7.40–7.10 (m, $ArCH_2$), 5.85–5.70 (m, $CH=CH_2$), 5.03–4.87 (dd, J_{cis} 10.0 Hz, J_{trans} 17.2 Hz $CH=CH_2$), 4.65 (m, CH_2Ar), 4.35 (NH-CH_2CH_2OCO-), 3.72 (N-CH_2CH_2OH), 3.61 (N-CH_2CH_2OH), 3.50–3.24 (m, CH_2-N), 2.80 (NH-CH_2CH_2OCO-), 2.42–2.10 (m, ACH_2ACONA), 2.05–1.95 (m, CH_2-$CH=CH_2$), 1.65–1.45 (m, -CH_2-CH_2-CO-), 1.43–1.20 (m, aliphatic backbone), 0.86 (t, ACH_3). ^{13}C NMR ($CDCl_3$, TMS, d in ppm): 173.8 (ACOANA), 139.2 (ACH¼CH_2), 136.4, 129.1, 128.7,

126.3 (Ar-CH_2-), 114.2 (-CH=CH_2), 58.6 (N-CH_2CH_2OH), 51.7 (N-CH_2CH_2OH), 45.3 (N-CH_2Ar), 33.8 (-CH_2CH=CH-), 33.4 (-CH_2CON-), 31.9 (-CH_2-CH_2-CH_3), 29.6–29.0 (aliphatic backbone), 25.4 (-CH_2CH_2CON-), 22.7 (-CH_2-CH_3), 14.4 (-CH_3).

Thiol-ene Polymer Modification

In a shlenck flask under argon, 2.1 g of polyoxazoline (1.5 mmol of 1a, 1b, or 1c; 2.0 mmol of 2a, 2b, or 2c; and 3.0 mmol of 3a, 3b, or 3c) was dissolved in 5 mL of anhydrous THF. DMPA (1% respect to the C=C) as initiator and mercaptoethanol (2.5 equiv. respect to the C=C) were added. The mixture was stirred and irradiated at 365 nm (18 W) for 2 h at room temperature. Excess reagent was removed by washing with brine several times, and the polymer was dried at 40 °C under vacuum for 48 h.

TABLE 1 Monomer Composition in the Feed and Molecular Weight of the Resulting Copolyoxazolines

Sample	I[a]	II[a]	I + II/BnBr ratio	M_n ($\times 10^{-3}$)[b]	M_n ($\times 10^{-3}$)[c]	M_n ($\times 10^{-3}$)[d]	DP[e]	M_n/M_w[d]
1a	0.15	0.85	8/1	1.70	2.09	2.24	11.2	1.08
1b	0.15	0.85	14/1	2.89	3.20	3.23	16.2	1.08
1c	0.15	0.85	20/1	4.09	4.12	4.09	20.5	1.11
2a	0.20	0.80	8/1	1.70	2.16	2.24	11.2	1.08
2b	0.20	0.80	14/1	2.90	3.25	3.28	16.4	1.08
2c	0.20	0.80	20/1	4.10	4.20	4.17	20.9	1.15
3a	0.30	0.70	8/1	1.71	1.97	2.21	11.0	1.08
3b	0.30	0.70	14/1	2.92	3.20	3.25	16.1	1.09
3c	0.30	0.70	20/1	4.12	4.40	4.20	20.9	1.13

[a] Molar percentage in the feed.
[b] Theoretical from the I+II/BnBr ratio.
[c] Determined by ^{1}H NMR.
[d] Determined by SEC using polystrene standards.
[e] Calculated from SEC results.

^{1}H NMR ($CDCl_3$, TMS, δ in ppm): 7.40–7.10 (m, $ArCH_2$), 4.65 (m, -CH_2Ar), 3.70 (t, CH_2-OH), 3.50–3.24 (m, CH_2-N), 2.71 (t, S-CH_2-CH_2OH-), 2.50 (t, -CH_2-S-CH_2CH_2OH), 2.40–2.10 (m, -CH_2CON-), 1.65–1.45 (m, -CH_2-CH_2-CON-),1.43–1.20 (m, aliphatic backbone), 0.86 (t, -CH_3). ^{13}C NMR ($CDCl_3$, TMS, δ in ppm): 173.9 (-CO-N-), 136.4, 129.1, 128.7, 126.3 (Ar-CH_2-), 60.5 (S-CH_2CH_2OH), 58.6 (N-CH_2CH_2OH), 51.7 (N-CH_2CH_2OH), 45.3 (N-CH_2Ar), 35.1 (S-CH_2CH_2OH), 33.4 (-CH_2CON-), 31.7 (-CH_2-CH_2-CH_3), 29.6–29.0 (aliphatic backbone), 25.5 (-H_2CH_2CON-), 22.7 (-CH_2-CH_3), 14.2 (-CH_3).

Polyurethane Synthesis

Around 2–3 g of polyol was dissolved under argon in the same weight of anhydrous toluene. The solution was heated at 50 °C and added to a 50% (w/w) dispersion of MDI in toluene. In all cases, a ratio of 1.02 equivalents of isocyanate group per hydroxyl was used. The mixture was stirred under argon until it become homogeneous and casted over silanized glass plaques preheated at 90 C. The polyurethane was maintained at 90 °C for 2 h and at 130 C for 3 h producing films with 0.03–0.04 mm thickness.

Determination of Hydroxyl Content

Quantification of the hydroxyl content was carried out using ^{1}H NMR spectroscopy and 2-phenylethanol as internal standard using the signal at 2.85 ppm as reference. Accurate weights of polyol and the internal standard were introduced in a NMR tube. The intensity of the partially overlapped signals at 3.79–3.70 ppm (side chain ACH_2OH and chain-end ACH_2OH groups) and the signal at 2.71 ppm (-S-CH_2-CH_2OH side chain groups) was compared with that of the intensity of the signals at 3.86 and 2.85 ppm (Ph-CH_2-CH_2-OH) of internal standard. The hydroxyl content in millimole of hydroxyl groups per gram of polyol was calculated using eq 1.

$$\text{value OH} = (\text{mmolIS} \times \text{IntPOH})/(\text{IntIS} \times \text{gPOH}) \qquad (1)$$

where mmolIS is the internal standard amount in mmol, IntPOH is the integral value of the polyol, IntIS is the integral value of the internal standard, and gPOH is the amount of polyol in grams.

Characterization

GC-mass spectrometry (GC-MS) analysis was done in a 6890N gas chromatograph and a 5973 mass spectrometer (Agilent Techologies, Palo Alto, CA), using a HP-5MS capillary column of 5% phenyl polydimethyl siloxane (30 m, 0.25 mm, 0.25 μm), from Agilent Technologies, and 99.999% pure helium gas as the carrier at a flow rate of 1.5 mL min^{-1}. Samples were injected in a split/splitless injector at a split ratio of 20:1, at a temperature of 280 °C. The oven temperature of GC was initially held at 60 °C, raised to 260 °C at a rate of 6 C min^{-1}, and then

held for 50 min. The mass spectrometer acquired data in scan mode with an m/z interval from 35 to 800. The compounds were identified by comparison with NIST08 MS library.

^{1}H NMR (400 MHz) and ^{13}C NMR (100.6 MHz) spectra were recorded in $CDCl_3$ using a Varian Gemini 400 spectrometer. Chemical shifts were reported in ppm relative to TMS as internal standard.

FTIR spectra were recorded on a Bomem Michelson MB 100 FTIR spectrophotometer with a resolution of 4 cm^{-1} in the absorbance mode. An attenuated total reflection (ATR) device with thermal control and a diamond crystal (Golden Gate heated single-reflection diamond ATR, Specac-Tknokroma) was used.

MALDI-TOF MS measurements were performed with a Voyager DE-RP mass spectrometer (Applied Biosystems, Framingham, MA) equipped with a nitrogen laser delivering 3 ns laser pulses at 337 nm. 1,8,9-Antracenetriol was used as matrix and potassium trifluoroacetate as dopant. Samples were prepared from a THF solution containing 40 mg/mL of matrix, 3 mg/mL of polymer, and 0.1 mg/mL of dopant. The homogenized mixture was casted in the MALDI plate.

Size exclusion chromatography (SEC) analysis was carried out with an Agilent 1200 series system with PLgel 3 lm MIXED-E, PLgel 5 µm MIXED-D, and PLgel 20 µm MIXED-A columns in series and equipped with an Agilent 1100 series refractive-index detector. Calibration curves were based on polystyrene standards having low polydispersities. THF was used as an eluent at a flow rate of 1.0 mL/min; the sample concentrations were 5–10 mg/mL, and injection volumes of 100 µL were used.

Calorimetric studies were carried out on a Mettler DSC822 differential scanning calorimeter using N_2 as a purge gas (20 mL/min). Dynamic mechanical thermal analysis (DMTA) and tensile tests were performed using a TA DMA 2928 in the controlled force–tension film mode with a preload force of 0.1 N, an amplitude of 10 µm, and at a fixed frequency of 1 Hz in the 80 to 170 C range and at a heating rate of 3 °C/ min. The tensile assays were performed in triplicates on rectangular samples (10 x 5 x 0.5 mm^3) measuring the strain while applying a ramp of 0.5 N/min at 25 °C. A preload force of 0.05 N and a soak time of 3 min were used. Thermal stability studies were carried out on a Mettler TGA/ SDTA851e/LF/1100 with N_2 as purge gas. The studies were performed in the 30–800 °C temperature range at a scan rate of 10 °C/min.

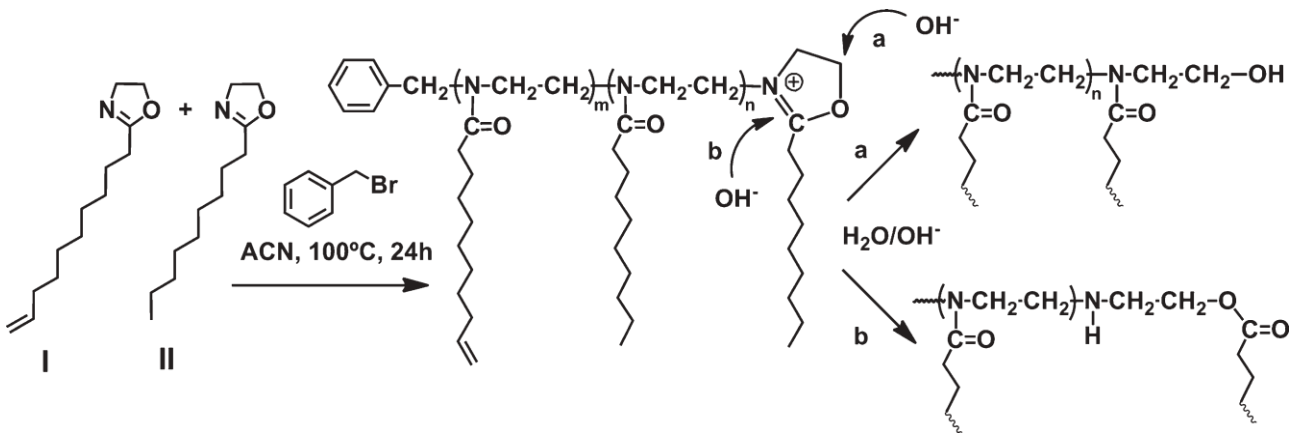

SCHEME 2 Cationic ring-opening copolymerization of oxazoline monomers and possible chain termination mechanisms.

RESULTS AND DISCUSSION

As commented, the main purpose of this work is preparing tailor-made thermosetting PUs from comb-like copoly-2-oxazolines functionalized with hydroxyl groups in the side chain. To prepare the starting 2-oxazoline monomers, we chose 10-undecenoic acid and decanoic acid as unsaturated and saturated precursors, respectively. Both starting materials are from renewable origin. 10-Undecenoic acid is the main product of castor oil caustic fusion or pyrolisis,[49] and decanoic acic occurs naturally in coconut and palm kernel oils and is the major component of eml seed oil (60–70%).[50] The synthesis of the 2-oxazoline monomers was accomplished using the standard two-step procedure consisting of the reaction of the acid with ethanolamine followed by treatment with thionyl chloride and basic hydrolysis[45–47] (Scheme 1).

The resulting 2-oxazolines were purified by fractional distillation under vacuum giving colorless oils in good yield (82% for I and 76% for II). Physical properties and structural characteristics were in accordance with those described in the literature.[31,47]

I was copolymerized with the necessary molar amount of II to obtain copolymers with a 15% (1 series), 20% (2 series), and 30% (3 series) of unsaturated comonomer (Table 1). The copolymerizations were carried out at 100 C in anhydrous ACN using benzyl bromide as initiator (Scheme 2).

Each mixture of monomer was polymerized using three different monomer/initiator ratios 8/1 (a series), 14/1 (b series), and 20/1 (c series). These initiator ratios were selected to obtain copolymers with a theoretical polymerization degree (DP) of 8, 14, and 20, respectively. In this way, nine different copolymers with varying compositions and molecular weights were obtained essentially with quantitative conversions. Results determined by SEC and ^{1}H NMR are collected in Table 1, together with the theoretical values expected from the monomer–initiator ratio used.

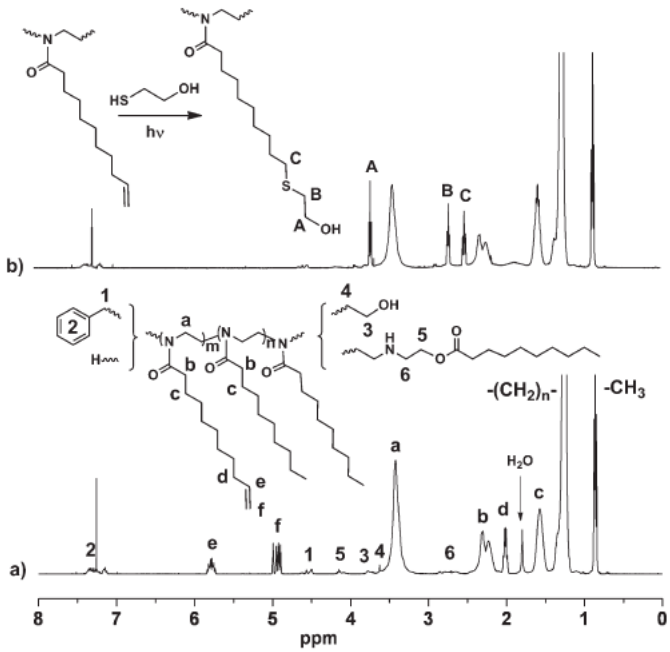

FIGURE 1 ^{1}H NMR spectra of (a) **2c** and (b) its thiol-ene addition product $\mathbf{2c_{OH}}$.

All copolymers were obtained in quantitative conversion and so the comonomer composition should match with the feed. The ^{1}H NMR spectra [(Fig. 1(a)] show the expected signals for copolymers obtained via a CROP initiated by benzyl bromide. In addition to the main and side chain proton signals of both comononer units, some other low intensity signals can be observed. These signals do not disappear or change their intensity by precipitating the polymer and so it can be assumed that they are due to end groups instead of polymer impurities. Signals between 7.40–7.12 ppm and 4.65–4.47 ppm can be assigned to the starting benzyl moieties whereas the signals at 3.77 and 3.63 ppm can be assigned to the final hydroxyethyl groups formed in the termination step by reaction with water. This was confirmed by ''in situ'' derivatization of the polymer with trichloroacetylisocyanate, which produces a downfield shift of 0.48 ppm for the signal at 3.77 ppm in the ^{1}H NMR spectrum. The relative intensity of signals at 4.65–4.47 ppm was used to estimate the molecular weight by comparing with the main chain methylene signal at 3.42 ppm. The signals at 4.15 and 2.90–2.60 ppm could be assigned to an ester end group, which can be formed alternatively by attack of water to the position 5 of the growing oxazolinium group as it has been established by Schubert and coworkers[51] (Scheme 2).

In all cases, SEC chromatograms of polymers (Fig. 2) show narrow monomodal distributions with polydispersities around 1.08 with the exception of the polymers obtained with 20/1 monomer/initiator ratio that presents a slightly higher polydispersity (1.11–1.15; Table 1). The M_n values obtained by SEC were somewhat higher than the theoretical ones taking into account the monomer/initiator ratio used. This behaviour is especially remarkable in the case of the low-molecular weight polymers.

Molecular weights estimated by ^{1}H NMR using the benzyl group signal were also higher than the theoretical ones because other existing initiations were not taken into account in the measurements. To gain insight about the structure of these polymers, MALDI-TOF-MS analysis was performed. In Figure 3(a), the representative spectrogram obtained for 2b is shown. In all samples, at least two different Gaussian peak distributions can be observed.

The main distribution fits with the expected structure for a random copolymer with benzyl and hydroxyl end groups and presents molecular weight distributions close to that observed by SEC. Each peak in the main distribution presents a fine structure which can be associated to the different comonomer composition as is shown in the expanded zone of the peak corresponding to DP 14 in Figure 3(b). As can be seen, the peaks of II_{14}, II_{13}/I_1, II_{12}/I_2 and up to II_7/ I_7 can be observed, by varying its relative intensity with the amount of II comonomer in the 3b. The same MALDI-TOFMS patterns are observed for 1 and 2 copolymer series. In all cases, a secondary peak distribution is observed. The mass of these secondary peaks fits with a random copolymer with hydrogen and hydroxyl end groups (difference of 91 Da with the main series peaks). These peaks can be explained on the basis of known chain transfer reactions that take place during the polymerization of

oxazolines[52] leading to hydrogen-initiated and enamine chains. Alternatively, these species can be formed as result of chain-transfer processes with traces of water or H-nucleophiles present in the polymerization media.[53] This secondary set of peaks follows the

same comonomer composition as that of the main peak series but not a Gaussian distribution. As expected, for species formed in chain-transfer processes, the peaks are more intense in the low-molecular weight region and its intensity decreases progressively as the DP increases. According to the relative peak intensity, the amount of chain transfer species is more important in 1c, 2c, and 3c compounds, which is in agreement with their wider molecular weight distribution observed by SEC. The presence of copolymer chains not initiated by benzyl groups also explains why the ^{1}H NMR molecular weight calculation gave higher values than the theoretical ones.

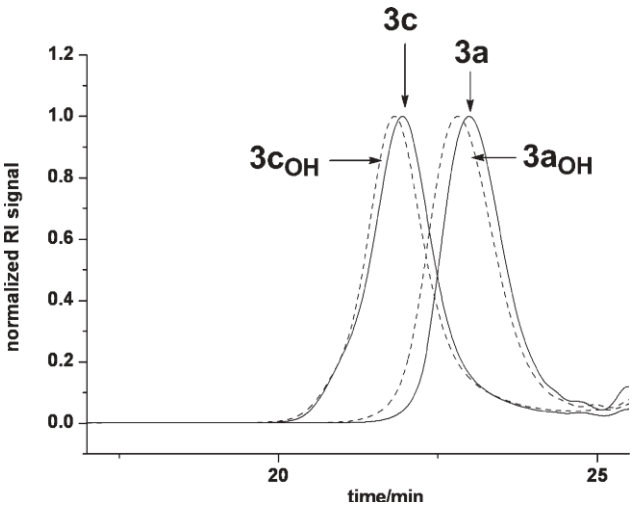

FIGURE 2 SEC chromatograms of 3a and 3c (continuous line) and the corresponding thiol-ene addition products 3a$_{OH}$ and 3c$_{OH}$ (dashed line).

We used photoinitiated thiol-ene addition of 2-mercaptoethanol to functionalize the pendant copolyoxazoline double bonds (Scheme 3 and Table 3).

After 2 h of irradiation, complete double bond conversion was achieved and the polyoxazoline-based poliols were obtained with simple work-up in quantitative yields. ^{1}H NMR analysis [Fig. 1(b)] show the absence of double bond signals and the appearance of three new signals at 2.51 ppm (-CH_2-S-CH_2CH_2-OH), 2.71 ppm (-CH_2-S-CH_2CH_2-OH), and 3.71 ppm (-CH_2-S-CH_2CH_2-OH) corresponding to the 2-hydroxyethylthioether group.

SEC analysis of polyoxazoline polyols (Fig. 2 and Table 2) show similar molecular weight distributions and polydispersities when compared with the starting unfunctionalized polyoxazolidine, thus indicating the absence of degradation and side chain processes.

MALDI-TOF-MS spectra show a complex pattern with several series of peaks separated by 78 mass units, which corresponds to the -CH_2-S-CH_2CH_2-OH moiety. These series of peaks could be assigned to the copolymers initiated with H and Bn groups and cationized either by sodium or potassium.

The hydroxyl number of all polyoxazoline–polyols was determined by ^{1}H NMR measuring the amount of hydroxyl end groups and side chain hydroxyl groups. The intensity of the signals at 3.80–3.70 ppm corresponding to side chain -CH_2OH and chain-end -CH_2OH groups were compared with the intensity of the signals at 3.86 and 2.85 ppm (Ph-CH_2-CH_2-OH) with a known amount of phenylethanol as internal standard. Also, the intensity of the signal at 2.71 ppm, corresponding to the -S-CH_2CH_2OH, was measured to calculate the hydroxyl content due exclusively to side chain groups. Both hydroxyl contents expressed in mmol of OH per gram of polymer are collected in Table 2. The calculated side chain hydroxyl values are in good agreement with the theoretical ones taking into account the copolymer composition thus confirming the efficiency of the functionalization under the mild conditions used. For each 3$_{PU}$, 3$_{PU}$, and 3$_{PU}$ polyol series, the total hydroxyl content increases as the molecular weight decreases due to the contribution of the chain end hydroxyl groups.

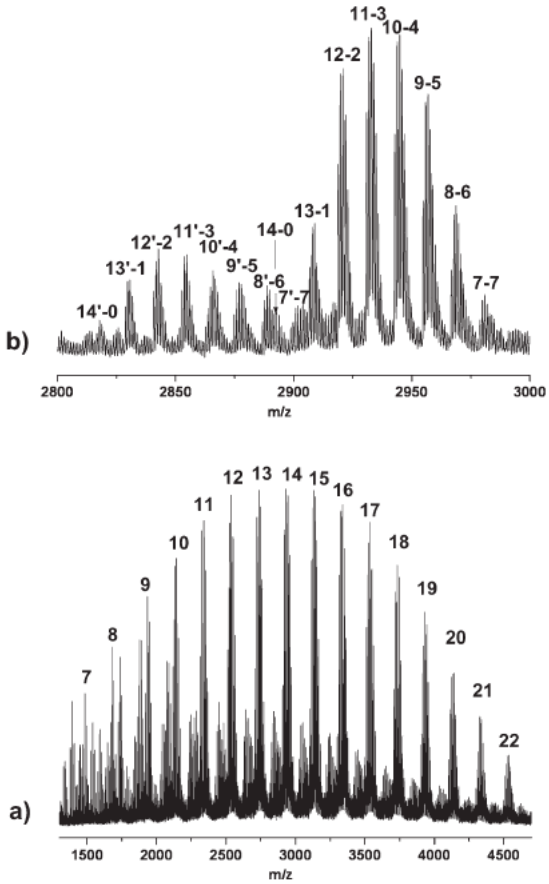

FIGURE 3 (a) MALDI-TOF-MS spectra of 3b, numbers indicate the DP. (b) Amplification of the peak corresponding to DP ¼ 14. Numbers indicate the copolymer composition: the first indicate the number of saturated monomeric units II and the second the number of unsaturated I ones. The series with apostrophe correspond to the polymers chains not initiated with benzyl groups.

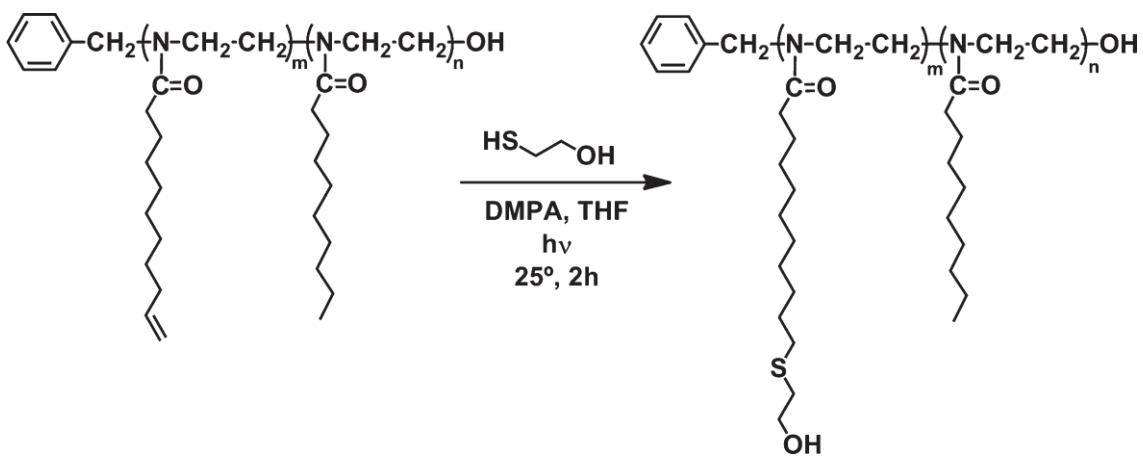

SCHEME 3 Functionalization of the copolyoxazolines by thiol-ene addition of 2-mercaptoethanol.

The resulting polyoxazolidine–polyols were yellowish clear waxy solids. DSC analysis shows its semicrystalline nature with glass transition temperature (T_g) values below 0 °C and multiple melting endotherms in the range of 50–100 °C (Table 2). Both, first- and second-order transitions increase with molecular weight for all copolymer series. Low-molecular weight copolyols showed a single melting endotherm

at about 50 °C whereas the rest of polyols show complex endotherms. According to results, the different thermal behavior of these samples seems to be related to the differences in molecular weight rather that to the hydroxyl group content.

These polyoxazoline-based polyols were used to prepare polyurethane thermosets by reaction with MDI in solution of toluene. In all cases, a slight excess of isocyanate group over the theoretical amount based on the total hydroxyl content of polyol was used. The PU prepolymers were casted onto glass plaques and cured at 130 °C for 3 h to produce flexible to hard yellowish transparent materials as films with 0.03–0.04 mm thickness. The synthesized polyols having primary hydroxyl groups showed an excellent compatibility with the MDI toluene suspension leading to homogeneous systems before the curing cycle.

FTIR analysis (Fig. 4) demonstrated the completion of the reaction by the disappearance of the band at 2240 cm^{-1} corresponding to the -N=C=O stretching of the isocyanate group and the appearance of the characteristic absorbances of the urethane links at 1728 cm^{-1}, which appears clearly differentiated from the band at 1641 cm^{-1} corresponding to the C=O stretching of the polyoxazoline amide groups. The C=O of these urethane linkages appears as a broad band between 1745 and 1690 cm^{-1} with a maximum at 1728 cm^{-1} and a shoulder at 1710 cm^{-1}, which are attributable to the associated and non-associated C=O urethane groups. No additional shoulders at about 1660 cm^{-1} attributable to urea linkages were observed. Moreover, the broad band centred at 3500 cm^{-1}, corresponding to the O-H stretching, shifts to lower frequencies and shows a maximum at 3315 cm^{-1}, characteristic of the N-H stretching of urethanes.

The thermal properties of polyurethanes were investigated by DSC (Fig. 5 and Table 3). The most significant feature is the appearance of a melting endotherm at 57–58 °C for PUs obtained from polyols of PUb with medium molecular weight (2900 Da) and PUc with high molecular weight (4100 Da).

TABLE 2 Molecular Weight, Hydroxyl Content, and Thermal Properties of the Polyoxazoline Polyols

Sample	$M_n \times 10^{-3}$ (M_n/M_w)[a]	mmolOH/g polyol[b]	mmolOH/g polyol[c]	T_g (°C)[d]	T_m (°C)[d]	ΔH (J/g)[d]
$\mathbf{1a}_{OH}$	2.34 (1.11)	0.79	1.22	−11.6	50.7	14.1
$\mathbf{1b}_{OH}$	3.41 (1.11)	0.80	1.08	−9.0	58.3, 81.0, 88.3	40.7
$\mathbf{1c}_{OH}$	4.31 (1.11)	0.80	0.89	−2.5	58.3, 87.3, 101.3	41.3
$\mathbf{2a}_{OH}$	2.42 (1.11)	1.08	1.45	−10.9	56.3	22.9
$\mathbf{2b}_{OH}$	3.57 (1.11)	1.09	1.34	−7.4	59.0, 84.3	40.6
$\mathbf{2c}_{OH}$	4.56 (1.16)	1.09	1.18	−3.6	58.3, 82.7, 93.7	41.9
$\mathbf{3a}_{OH}$	2.50 (1.10)	1.20	1.66	−11.7	54.7	21.1
$\mathbf{3b}_{OH}$	3.62 (1.11)	1.23	1.47	−6.6	57.7, 78,7	40.1
$\mathbf{3c}_{OH}$	4.58 (1.14)	1.21	1.32	−3.9	60.3, 84.7	41.8

[a] Determined by SEC using polystrene standards.
[b] Side chain OH content determined by ^{1}H NMR.
[c] Side chain plus chain-end OH content determined by ^{1}H NMR.
[d] Determined by DSC.

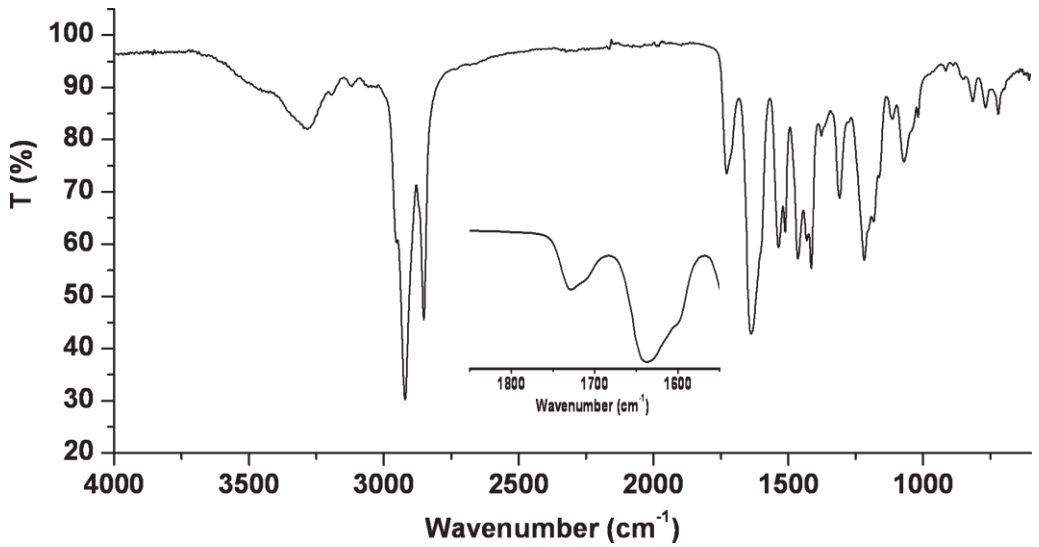

FIGURE 4 FTIR-ATR spectrum of $2c_{PU}$.

In these cases, the crystallinity is higher for the PUs obtained from the higher molecular weight polyoxazoline polyols. When comparing PUs obtained from polyols of the same molecular weight but increasing hydroxyl content ($1b_{PU}$, $2b_{PU}$, $3b_{PU}$ and $1c_{PU}$, $2c_{PU}$, $3c_{PU}$ series), a

decrease in its relative crystallinity degree is observed which can be related to the increasing difficulty in the chain packing as the crosslinking degree increases.

The T_g for all PUs is around 20 °C showing a slight increase with the starting polyol molecular weight in series 1_{PU} and 2_{PU} but not in the case of series 3_{PU}. This complex behavior can be related with the occurrence of two different effects. Lower molecular weight polyols have higher hydroxyl content and consequently leads to PUs with higher number of urethane links; however, PUs from high-molecular weight polyols have crystalline regions that act as physical crosslinking restricting mobility. In the absence of other effects, PUs made from polyols of similar molecular weight but increasing hydroxyl content, should lead to an increase in the number of urethane links and consequently in the T_g values. This behavior is effectively observed in PUs obtained from similar comb-like amorphous polyetherpolyols.[15] In this case, it must be considered that the semicrystalline nature of these PUs and the fact that the strong polar interactions between the amide groups can be disrupted as the amount of urethane links increases. This consideration is supported by the fact that polyoxazoline–polyols with the similar molecular weight but different hydroxyl content (i.e., $1c_{OH}$, $2c_{OH}$, and $3c_{OH}$) have very close T_g values (Table 2).

The thermal stability of polyurethanes was studied in N_2 atmosphere (Table 3). The shapes of the weight-loss curves were very similar for all PUs and differences in the thermal stability seem to be negligible. The decomposition shows three main stages for most of the PUs [Fig. 6(a)]. The first has a maximum that increases from 219 °C to 272 °C in the 2_{PU} series and from 233 °C to 252 °C in the 3_{PU} series in a parallel way with the increase of molecular weight of the starting polyol. The associated weight loss (5–10% of the total mass) decreases with the same parameter and so this decomposition process can be associated in part to the parent polyol moiety fragmentation. This can be inferred when comparing the TGA curves of a PU, its parent polyol and the original polyoxazoline [(Fig. 6(b)]. As can be seen, all polymers have a main degradation process with a maximum around 400 °C, but the polyoxazoline polyol and the polyurethane present an additional low temperature degradation process that is not observed in the polyoxazolidine polymer. This seems to indicate that this degradation process is related in part with the cleavage of the -S-CH_2-CH_2-O- moieties.

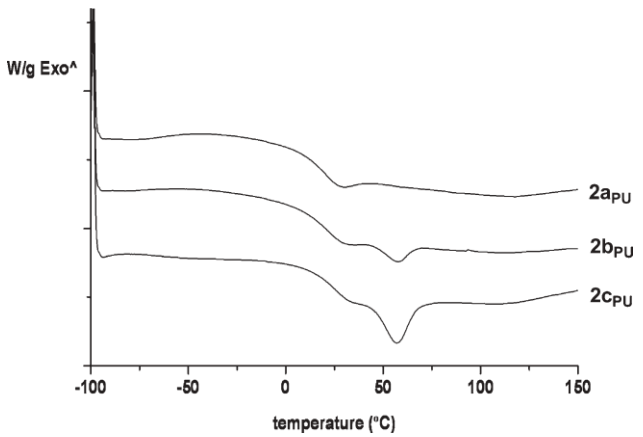

FIGURE 5 Second heating DSC traces of $2a_{PU}$, $2b_{PU}$, and $2c_{PU}$.

TABLE 3 Thermal and Mechanical Properties of Pus

	T_g (°C)		T_m		TGA (N_2)	DMTA		
Sample	$\frac{1}{2}\ \Delta C_p$[a]	tan δ_{max}[b]	T_{max} (°C)[a]	ΔH (J/g)[a]	T_{max} (°C)	Young's Modulus (MPa)	Stress (MPa)	Strain (%)
$1a_{PU}$	12	49	–	–	224, 335, 415	6	2.2	177
$1b_{PU}$	20	56	58	8.3	338, 413	85	9.3	76
$1c_{PU}$	26	64	58	9.7	338, 414	254	14.3	25
$2a_{PU}$	20	51	–	–	219, 334, 410	6	3.1	268
$2b_{PU}$	21	50	57	2.9	238, 333, 410	41	6.2	94
$2c_{PU}$	23	53	57	6.1	272, 337, 410	46	7.9	83
$3a_{PU}$	24	52	–	–	233, 338, 411	8	4.5	229
$3b_{PU}$	21	51	–	–	246, 340, 409	13	5.3	163
$3c_{PU}$	18	48	58	1.8	252, 336, 410	29	8.0	160

[a] Determined by DSC.

[b] Determined by DMTA.

The second degradation step has a maximum at 335–340 °C for all samples and can be associated to the initial decomposition of the urethane links. The third and main decomposition step has a maximum at 410–415 °C for all PUs and supposes the complete degradation of the polyoxazoline and urethane moieties leading to a carbonaceous residue of about 1% of the initial weight in all cases.

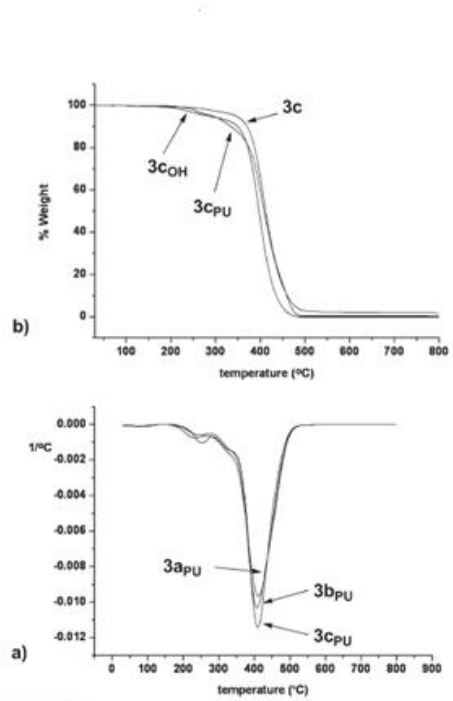

FIGURE 6 (a) First derivative curve of the TGA plots of 3a$_{PU}$, 3b$_{PU}$, and 3c$_{PU}$. (b) TGA plots of 3c, 3c$_{OH}$, and 3c$_{PU}$.

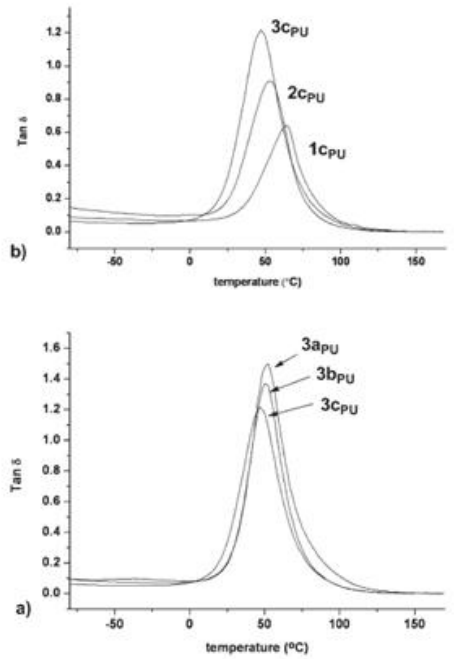

FIGURE 7 Variation of tan δ peak of PUs with (a) the molecular weight of the parent polyol (3a$_{PU}$, 3b$_{PU}$, and 3c$_{PU}$) and (b) with the hydroxyl content of the parent polyol (1c$_{PU}$, 2c$_{PU}$, and 3c$_{PU}$).

The dynamomechanical behavior of PUs was studied by DMTA. Typical DMTA plots for crosslinked polymeric networks were observed in all cases. A glassy state with a high modulus plateau E′ at lower temperatures and a rubbery state with lower E′ at higher temperatures is observed. For all PU series, the storage moduli at the rubbery plateau slightly increases with the molecular weight of the starting polyol. PUs behave like homogeneous networks with a unique broad transition that according to DSC corresponds to the glass transition in the amorphous PU and the glass transition and melting in the semicrystalline PUs.

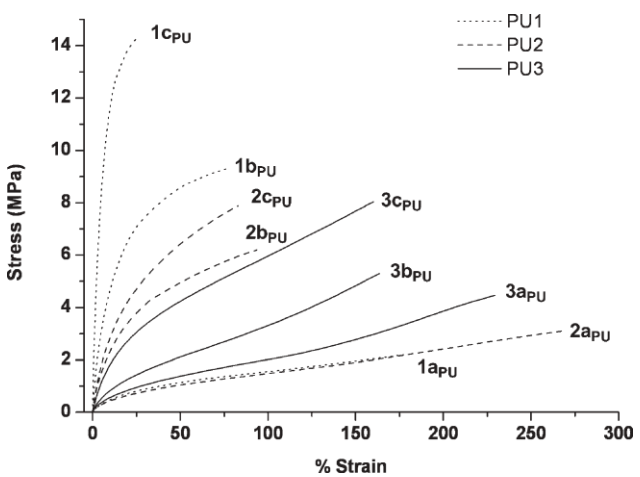

FIGURE 8 Stress–strain plots of all PUs.

Figure 7(a,b) shows the representative tan d of some synthesized PUs. Consistent with DSC results, this peak shows a slight shift of maxima when increasing the molecular weight of the parent polyol for series 1_{PU} and 2_{PU}, which is consistent with the increase in its crystallinity degree. In the case of PU3 series that are practically amorphous, a slight decrease of the maxima is observed [Fig. 7(a)]. The variation of the tan d peak when comparing 1_{PU}, 2_{PU}, and 3_{PU} series [Fig. 7(b)] is also consistent with the decrease in the crystalline content as the functionality of the parent polyol increases. These results seem to indicate that mechanical properties of these PUs are mostly governed by their crystalline content, which is directly related to the molecular weight of the parent polyol, instead of the amount of urethane links introduced.

Figure 8 shows the stress–strain curves, and Table 3 summarizes the mechanical properties of obtained PUs. Young's modulus and tensile strength at break increase as the molecular weight of the parent polyol increases for all series. As expected, an enhancement of the modulus and tensile strength can be observed when increasing the semicrystalline nature of the PUs. What is most notable is the high modulus of $1c_{PU}$ that is consistent with its high crystalline degree and its maximum T_g and tan δ values determined, respectively, by DSC and DMTA.

CONCLUSIONS

The transformation of saturated and unsaturated fatty acids in oxazoline monomers is a straightforward and convenient methodology to produce polymers with controlled molecular weight, composition, and end group functionality using CROP. The side chain unsaturated groups can be effectively and quantitatively functionalized, under mild conditions using the thiol-ene addition of mercaptoethanol, to produce renewable polyoxazoline–polyols. These polyols have preset characteristics that can be used to prepare PUs with tailored characteristics ranging from hard-rigid to soft-elastic materials.

The authors express their thanks to MICINN (Comision Interministerial de Ciencia y Tecnologia) (MAT2008-01412) for financial support for this work.

REFERENCES AND NOTES

1 Belgacem, M. N.; Gandini, A. Monomers, Polymers and Composites from Renewable Resources; Elsevier: Oxford, 2008.

2 Guner, F. S.; Yagci, Y.; Erciyes, A. T. Prog Polym Sci 2006, 31, 633–679.

3 Meier, M. A. R.; Metzger, J. O.; Shubert, U. S. Chem Soc Rev 2007, 36, 1788–1802.

4 (a) Sharma, V.; Kundu, P. P. Prog Polym Sci 2008, 33, 1199–1215; (b) Sharma, V.; Kundu, P. P. Prog Polym Sci 2006, 31, 983–1008.

5 Xia, Y.; Larock, R. C. Green Chem 2010, 12, 1893–1909.

6 Biermann, U.; Friedt, W.; Lang, S.; Luhs, W.; Machmuller, G.; Metzger, J. O.; Klaas, G.; Rusch, M.; Schafer, H. J.; Schneider, M. P. Angew Chem Int Ed Engl 2000, 39, 2206–2224.

7 Petrovic, Z. S. Polym Rev 2008, 48, 109–155.

8 Lligadas, G.; Ronda, J. C.; Galia, M.; Cadiz, V. Biomacromolecules 2010, 11, 2825–2835.

9 Harry-O'kuru, R. E.; Holster, R. A.; Abbott, T. P.; Weisleder, D. Oil Ind Crop Prod 2002, 15, 51–58.

10 Guo, Y.; Hardesty, J. H.; Mannri, V. M.; Massingill, J. J. L. J Am Oil Chem Soc 2007, 84, 928–935.

11 Gryglewicz, S.; Piechocki, W.; Gryglewicz, G. Bioresour Technol 2003, 87, 35–39.

12 Campanella, A.; Bonnaillie, L. M.; Wool, R. P. J Appl Polym Sci 2009, 112, 2567–2578.

13 Petrovic, Z. S.; Guo, A.; Javni, I.; Biomacromolecules 2005, 6, 713–719.

14 Petrovic, Z. S.; Guo, A.; Javni, I.; Cvetkovic, I.; Hong, D. P. Polym Int 2008, 57, 275–281.

15 Lligadas, G.; Ronda, J. C.; Galia, M.; Biermann, U.; Metzger, J. O. J Polym Sci, Part A: Polym Chem 2006, 44, 634–645.

16 del Rio, E.; Galia, M.; Cadiz, V.; Lligadas, G.; Ronda, J. C. J Polym Sci Part A: Polym Chem 2010, 48, 4995–5008.

17 del Rio, E.; Lligadas, G.; Ronda, J. C.; Galia, M.; Cadiz, V. J Polym Sci Part A: Polym Chem 2010, 48, 5009–5017.

18 Kobayashi, S.; Uyama, H. J Polym Sci Part A: Polym Chem 2002, 40, 192–209.

19 Hoogenboom, R. Macromol Chem Phys 2007, 208, 18–25.

20 Park, J.-S.; Kataoka, K. Macromolecules 2007, 40, 3599–3609.

21 Fijten, M. W. M.; Kranenburg, J. M.; Thijs, H. M. L.; Paulus, R. M.; van Lankvelt, B. M.; de Hullu, J.; Springintveld, M.; Thielen, D. J. G.; Tweedie, C. A.; Hoogenboom, R.; van Vliet, K. J.; Schubert, U. Macromolecules 2007, 40, 5879–5886.

22 Fijten, M. W. M.; Hoogenboom, R.; Schubert, U. J Polym Sci, Part A: Polym Chem 2008, 46, 4804–4816.

23 Weber, C.; Becer, C. R.; Baumgaertel, A.; Hoogenboom, R.; Schubert, U. Design Monom Polym 2009, 12, 149–165.

24 Kempe, K.; Jacobs, S.; Lambermont-Thijs, H. M. L.; Fijten, M. W. M.; Hoogenboom, R.; Schubert, U. Macromolecules 2010, 48, 5533–5540.

25 Aoi, K.; Okada, M. Prog Polym Sci 1996, 21, 151–208.

26 Zhou, P.; Blubaum, J. E.; Burns, C. T.; Natale, N. R. Tetrahedron Lett 1997, 38, 7019–7020.

27 Bandgar, B. P.; Pandit, S. S. Tetrahedron Lett 2003, 44, 2331–2333.

28 Stefano, C.; Abigail, Y.; Bruno, L.; Tetrahedron Lett 2004, 45, 9611–9615.

29 Hioki, K.; Takechi, Y.; Kimura, N.; Tanaka, H.; Kunishima, M. Chem Pharm Bull 2008, 56, 1735–1737.

30 Kempe, K.; Lobert, M.; Hoogenboom, R.; Schubert, U. S. J Comb Chem 2009, 11, 274–280.

31 Cai, G.; Litt, M. H. J Polym Sci Part A: Polym Chem 1996, 34, 2679–2688.

32 Cai, G.; Litt, M. H.; J Polym Sci Part A: Polym Chem 1996, 34, 2701–2709.

33 Hoogenboom, R.; Wiesbrock, F.; Huang, H.; Leenen, M. A. M.; Thijs, H. M. L.; van Nispen, S. F. G. M.; van der Loop, M.; Fustin, C.-A.; Jonas, A. M.; Gohy, J.-F.; Schubert, U. S. Macromolecules 2006, 39, 4719–4725.

34 Chung, T. C.; Raate, M.; Berluche, E.; Schulz, D. N. Macromolecules 1988, 21, 1903–1907.

35 Eroglu, M. S.; Hazer, B.; Ozturk, T.; Caykara, T. J Appl Polym Sci 2005, 97, 2132–2139.

36 Cai, G.; Litt, M. H. J Polym Sci Part A: Polym Chem 1996, 34, 2711–2717.

37 Cai, G.; Litt, M. H. J Polym Sci Part A: Polym Chem 1996, 34, 2689–2699.

38 Hoyle, C. E.; Bowman, C. N. Angew Chem Int Ed Engl 2010, 49, 1540–1573.

39 Hoyle, C. E.; Lowe, A. B.; Bowman, C. N. Chem Soc Rev 2010, 39, 1355–1387.

40 Lluch, C.; Ronda, J. C.; Galia`, M.; Lligadas, G.; Ca´diz, V. Biomacromolecules 2010, 11, 1646–1653.

41 Luxenhofer, R.; Jordan, R. Macromolecules 2006, 39, 3509–3516.

42 Gress, A.; Volkel, A.; Schlaad, H. Macromolecules 2007, 40, 7928–7933.

43 Diehl, C.; Schlaad, H. Macromol Biosci 2009, 9, 157–161.

44 Cortez, M. A.; Grayson, S. M. Macromolecules 2010, 43, 4081–4090.

45 Culbertson, B. M. Prog Polym Sci 2002, 27, 579–626.

46 Holerca, M. N.; Percec, V. Eur J Org Chem 2000, 2257–2263.

47 Moaddel, H.; Ameri, R. Iranian Polym J 2005, 14, 849–854.

48 Jordan, R.; Martin, K.; Arder, H. J.; Unger, K. K. Macromolecules 2001, 34, 8858–8865.

49 Van der Steen, M.; Stevens, C. V. ChemSusChem 2009, 2, 692–713.

50 Badami, R. C.; Patil, K. B. Prog Lipid Res 1981, 19, 119–153.

51 Baumgaertel, A.; Altuntas, E.; Kempe, K.; Crecelius, A.; Schubert, U. S. J Polym Sci Part A Polym Chem 2010, 48, 5533–5540.

52 Wiesbrock, F.; Hoogenboom, R.; Leenen, M.; van Nispen, S. F. G. M.; van der Loop, M.; Abeln, C. H. C. H.; van der Berg, A. M. J.; Schubert, U. S. Macromolecules 2005, 38, 7957–7966.

53 Warakomski, J. M.; Thill, B. P. J Polym Sci Part A: Polym Chem 1990, 28, 3551–3563.